JOURNAL OF BACTERIOLOGY, Aug. 2007, p. 6011–6020 Vol. 189, No. 16
0021-9193/07/$08.00+0 doi:10.1128/JB.00014-07

Quorum Sensing in *Escherichia coli* Is Signaled by AI-2/LsrR: Effects on Small RNA and Biofilm Architecture▽†

Jun Li,[1,3] Can Attila,[5] Liang Wang,[1,4] Thomas K. Wood,[5] James J. Valdes,[6] and William E. Bentley[1,2,3]*

Center for Biosystems Research, University of Maryland Biotechnology Institute,[1] Fischell Department of Bioengineering,[2] Department of Chemical and Bimolecular Engineering,[3] and Department of Cell Biology and Molecular Genetics,[4] University of Maryland, College Park, Maryland 20742; Department of Chemical Engineering, Texas A&M University, College Station, Texas[5]; and Army Edgewood Chemical Biological Center, Aberdeen Proving Ground, Maryland 21010[6]

Received 3 January 2007/Accepted 28 May 2007

The regulatory network for the uptake of *Escherichia coli* autoinducer 2 (AI-2) is comprised of a transporter complex, LsrABCD; its repressor, LsrR; and a cognate signal kinase, LsrK. This network is an integral part of the AI-2 quorum-sensing (QS) system. Because LsrR and LsrK directly regulate AI-2 uptake, we hypothesized that they might play a wider role in regulating other QS-related cellular functions. In this study, we characterized physiological changes due to the genomic deletion of *lsrR* and *lsrK*. We discovered that many genes were coregulated by *lsrK* and *lsrR* but in a distinctly different manner than that for the *lsr* operon (where LsrR serves as a repressor that is derepressed by the binding of phospho-AI-2 to the LsrR protein). An extended model for AI-2 signaling that is consistent with all current data on AI-2, LuxS, and the LuxS regulon is proposed. Additionally, we found that both the quantity and architecture of biofilms were regulated by this distinct mechanism, as *lsrK* and *lsrR* knockouts behaved identically. Similar biofilm architectures probably resulted from the concerted response of a set of genes including *flu* and *wza*, the expression of which is influenced by *lsrRK*. We also found for the first time that the generation of several small RNAs (including DsrA, which was previously linked to QS systems in *Vibrio harveyi*) was affected by LsrR. Our results suggest that AI-2 is indeed a QS signal in *E. coli*, especially when it acts through the transcriptional regulator LsrR.

Bacteria communicate with each other through small "hormone-like" organic molecules referred to as autoinducers. Autoinducer-based bacterial cell-to-cell communication, enabling population-based multicellularity, has been termed quorum sensing (QS) (27). Cellular functions controlled by QS are varied and reflect the needs of a particular bacterial species for inhabiting a given niche (10, 38, 65).

QS among *Escherichia coli* and *Salmonella* strains has been a topic of great interest, and different intercellular signaling systems have been identified: that mediated by the LuxR homolog SdiA; the LuxS/autoinducer 2 (AI-2) system, an AI-3 system, and a signaling system mediated by indole (2, 19, 36, 57, 61, 68). Among these systems, the LuxS/AI-2 system possesses the unique feature of endowing cell population-dependent behavior while interacting with central metabolism through the intracellular activated methyl cycle (20, 21, 45, 65, 73). Therefore, it has the potential to influence both gene regulation and bacterial fitness.

AI-2's function has been studied using *luxS* mutants and by adding either conditioned medium or in vitro-synthesized AI-2 to bacterial cultures. It is noteworthy that the *luxS* transcription profile is not synchronous with the accumulation profile of extracellular AI-2 in bacterial supernatants (5, 31, 75). In *E. coli*, extracellular AI-2 activity peaks during the mid- to late-exponential phase and rapidly decreases during entry into the stationary phase. A corresponding decrease in LuxS protein levels is not observed (31, 75). The disappearance of extracellular AI-2 activity in *E. coli* and *Salmonella enterica* serovar Typhimurium is due to its uptake, carried out by its import through an ATP-binding cassette (ABC) transporter named the *luxS*-regulated (Lsr) transporter (62, 69, 75). The transporter proteins are part of the *lsr* operon, which is regulated by cyclic AMP/cyclic AMP receptor protein and proteins transcribed from two genes, *lsrK* and *lsrR*, located immediately upstream of *lsr* and divergently transcribed in its own *lsrRK* operon (70). The cytoplasmic kinase LsrK phosphorylates AI-2 into an activated molecule that is suggested to bind and derepress the *lsr* repressor LsrR. A conceptual model of the LsrR/phospho-AI-2 circuit is provided in Fig. 1.

LsrR and LsrK were among the first positively identified QS regulators in *E. coli* (19, 70, 75). Since QS regulators are responsible for mediating many cellular phenotypes and morphologies (18, 30, 34), the functions of LsrR and LsrK are of great interest. Furthermore, it is well known that AI-2 uptake is an integral part of the *E. coli* QS network; thus, it remains intriguing that these bacteria actively transport its QS autoinducer. In many other systems, the signal molecule is freely diffused or binds a cognate receptor, triggering a sensor-kinase couple. It is possible that AI-2-signaling bacteria import and internalize AI-2 to terminate extracellular AI-2-dependent cellular responses and alternatively trigger cytoplasmic AI-2-dependent gene expression, akin to a genetic switching mechanism.

The physiological functions associated with either extracellular

* Corresponding author. Mailing address: Center for Biosystems Research, University of Maryland Biotechnology Institute, College Park, MD 20742. Phone: (301) 405-4321. Fax: (301) 314-9075. E-mail: bentley@eng.umd.edu.

† Supplemental material for this article may be found at http://jb.asm.org/.

▽ Published ahead of print on 8 June 2007.

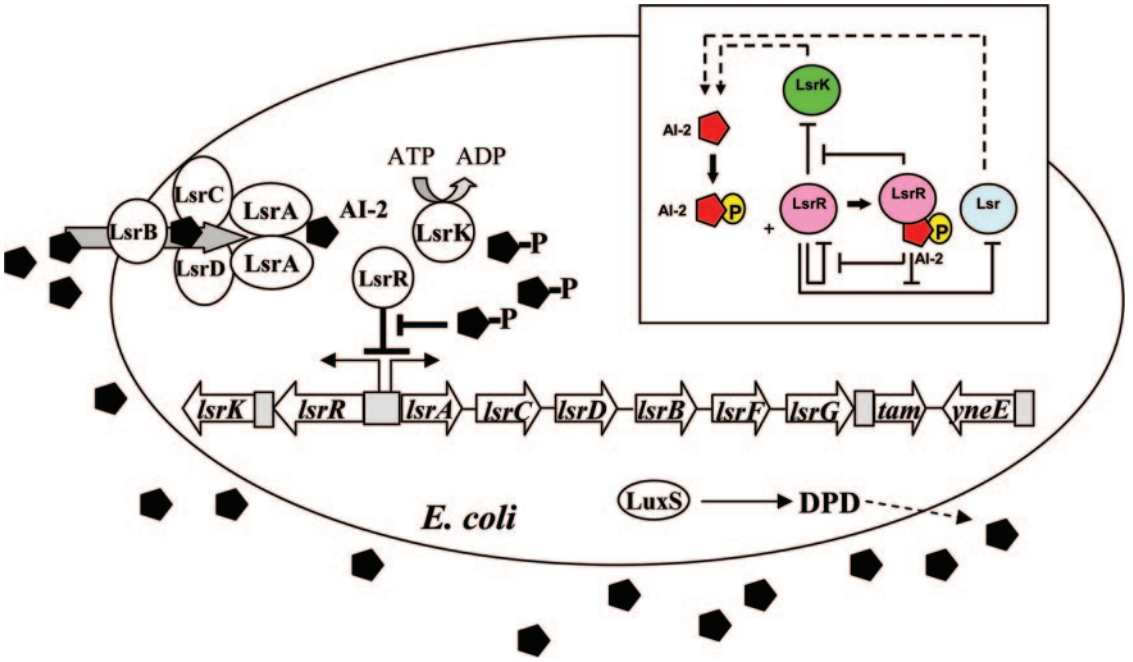

FIG. 1. Regulatory mechanisms of the LsrR/phospho-AI-2 circuit in *E. coli* AI-2 uptake (modified from reference 70). The AI-2 uptake repressor LsrR represses many genes including the *lsr* operon (comprised of *lsrACDBFG*) and the *lsrRK* operon. AI-2 can be imported back inside the cell via LsrACDB. Imported AI-2 is processed as phospho-AI-2 via the kinase LsrK. Phospho-AI-2 has been reported to bind LsrR and relieve its repression of the *lsr* transporter genes, triggering their expression. This in turn stimulates additional AI-2 uptake. DPD, 4,5-dihydroxy-2,3-pentanedione.

or cytoplasmic AI-2 can be partially revealed using *lsrK* and *lsrR* mutants. In *lsrK* mutants, Lsr transporter expression is repressed, and AI-2 remains in the supernatant (extracellular AI-2) (69). In *lsrR* mutants, the Lsr transporter is expressed, and extracellular AI-2 is continuously imported into the cell (cytoplasmic AI-2), irrespective of its accumulation (62, 69). We carried out genome-wide transcriptome analyses of *lsrR* and *lsrK* mutants relative to the isogenic parent strain W3110. We further evaluated physiological changes (biofilm formation, motility, etc.) resulting from the mutations. We found that *lsrR* and *lsrK* serve as global regulators of gene expression and affect biofilm architecture through the coordinate regulation of biofilm-related genes such as *wza* (responsible for colanic acid) and the autoaggregation gene *flu*. While the expression of many important genes was found to be altered by *lsrR* and *lsrK* deletions (and are putatively regulated by LsrRK), those associated with host invasion, stress responses, and foreign DNA were most prevalent. For the first time, small riboregulators were shown to respond to the QS regulators *lsrR* and *lsrK*. Finally, and perhaps most importantly, our results suggest that *lsrR* and *lsrK* (or, more specifically, LsrR and AI-2) operate in tandem and in the inverse of their role in regulating AI-2 uptake. Positive identification of LsrR/AI-2 signaling sheds new light on the widely discussed differences between AI-2, the metabolic by-product, and AI-2, the QS signaling molecule (70, 73).

MATERIALS AND METHODS

Bacterial strains and growth conditions. *E. coli* K-12 strain W3110 (F^- λ^- in *rrnD-rrnE*) was obtained from the Genetic Stock Center (New Haven, CT). Details of its kanamycin-resistant isogenic mutants used in this study, W3110 Δ*lsrR* and W3110 Δ*lsrK*, were described elsewhere previously (69). *E. coli* strain ZK2686 [W3110 Δ(*argF-lac*)*U169*] and its isogenic *agn43* mutant ZK2692 (ZK2686 *agn43*::*cam*) were kindly provided by R. Kolter (16). Luria-Bertani broth (LB) contains 5 g $liter^{-1}$ yeast extract (Difco), 10 g $liter^{-1}$ Bacto tryptone (Difco), and 10 g $liter^{-1}$ NaCl. Cultures of *E. coli* (wild type and Δ*lsrR* and Δ*lsrK* mutants) grown overnight in LB were diluted to an optical density at 600 nm (OD_{600}) of ~0.03 in LB and subsequently incubated at 30°C and 250 rpm in two 50-ml shake flasks. When the cultures reached the appropriate OD_{600} (2.4), the cells were harvested for RNA extraction.

RNA isolation, cDNA generation, and microarray processing. Total RNA was isolated using RNeasy Mini kits (QIAGEN Inc., Valencia, CA) according to the manufacturer's instructions. cDNA was synthesized and labeled according to the manufacturer's suggestions for *E. coli* Antisense genome arrays (Affymetrix Inc., Santa Clara, CA). Further preparation, hybridization, and scanning were carried out as previously described (70). Reverse transcription (RT)-PCR was also performed as previously reported (70), except that an Applied Biosystems 7300 real-time PCR system (Applied Biosystems) was used. 16S rRNA was used for normalizing all reactions; its transcript levels showed minimal variation between wild-type and mutant cells (data not shown).

Microarray data analysis. Microarray data were analyzed with the Affymetrix Microarray Suite software 5.1 (Affymetrix Inc., Santa Clara, CA) and a four-comparison survival method (15). The fluorescence of each array was normalized by scaling total chip fluorescence intensities to a common value of 500. For each growth condition, two independent experimental cell cultures (wild type) were compared with two independent control groups (Δ*lsrR* or Δ*lsrK* mutant), and four comparisons were made. The change (*n*-fold) for each gene was calculated by dividing the signal intensity for these two mutants by the signal intensity for the wild type. The reported values for the change (*n*-fold) are the averages of the four comparisons. Genes with consistent increases or decreases in all comparisons were determined and used for the analysis. However, the induced genes with absent calls of the array signal in the experimental groups and the repressed genes with absent calls of the array signal in the control groups were eliminated. Determinations of functional categories were based on the *E. coli* K-12 MG1655 database from TIGR (http://www.tigr.org/tigr-scripts/CMR2/gene_table.spl?db=ntec01).

SEM. Cells were collected and gently washed three times with Millonig's phosphate buffer (pH 7.3) (centrifugation at 2,000 × *g* for 10 min) and fixed with 2% glutaraldehyde (1 h at room temperature and 9 h at 4°C). Cells were collected with 0.2-μl filters, and residual glutaraldehyde was washed out using Millonig's phosphate buffer three times before cells were further fixed in 1% OsO_4. The filters were then dehydrated with ethanol (70%, 95%, and 100%).

The filters were fully dehydrated in a Denton vacuum freezer (Denton DCP-1 critical-point dryer) and coated with Ag-Pd (Denton DV 502/503 vacuum evaporator). Coated filters were examined by scanning electron microscopy (SEM) at the Biological Ultrastructure Laboratory of the University of Maryland (College Park, MD).

Autoaggregation assay. Autoaggregation assays were performed as described previously (32), with slight modifications. Cultures grown overnight were adjusted to the same optical densities, and 10 ml of each culture was placed into a 15-ml Falcon tube and kept on ice. At each time point, 100-μl samples were taken from each tube, ~1 cm from the top, and transferred into new tubes containing 1 ml 0.9% NaCl for measuring optical densities.

Flow cell biofilm experiments and image analysis. *E. coli* K-12 W3110 cells constitutively expressing green fluorescent protein via pCM18 were streaked onto LB agar plates with erythromycin (300 μg/ml) and grown in the same medium overnight. *E. coli* K-12 W3110 Δ*lsrK*:Kan^r/pCM18 and *E. coli* K12 W3110 Δ*lsrR*:Kan^r/pCM18 were streaked onto LB agar plates with erythromycin (300 μg/ml) and kanamycin (50 μg/ml) and then grown overnight in the same medium. Cultures grown overnight were diluted into LB and erythromycin (300 μg/ml) to reach an OD_{600} of 0.05. The flow cell (22) was inoculated for 2 h at 30°C with 200 ml of these cells, and fresh medium was then added at a flow rate of 10 ml/h for 49 h. The number of cells in the culture after 2 h of inoculation was 1.4×10^5 to 3.2×10^5 cells/ml. For the wild-type strain, biofilm formation was not significant at 24 h, so only images at 49 h were taken for all three strains. Green fluorescent protein was visualized by excitation with an Ar laser at 488 nm (emission, 510 to 530 nm) using a TCS SP5 scanning confocal laser microscope with a 63× HCX PL FLUOTAR L dry objective with a correction collar and a numerical aperture of 0.7 (Leica Microsystems, Mannheim, Germany). Color confocal flow cell images were converted to gray scale using an Image Converter (Neomesh Microsystems, Wainuiomata, Wellington, New Zealand). Biomass, substratum coverage, surface roughness, and mean thickness were determined using COMSTAT image-processing software (22) written as a script in Matlab 5.1 (The MathWorks) and equipped with the Image Processing Toolbox. Thresholding was fixed for all image stacks. At each time point, nine different positions were chosen for microscope analysis, and 225 images were processed for each position. Values are means of data from the different positions at the same time point, and standard deviations were calculated based on these mean values for each position. Reconstructed three-dimensional images were obtained using IMARIS (BITplane, Zurich, Switzerland). Twenty-five pictures were processed for each three-dimensional image.

RESULTS

Deletion of *lsrR* and *lsrK* does not affect growth or motility. We observed no changes in growth rate and cell motility due to a deletion of either *lsrR* or *lsrK* when cells were grown in LB (data not shown). No significant differences in biofilm formation were found using a crystal violet assay for cells cultivated up to 24 h in various media (data not shown). We then used SEM to visualize biofilm morphology. W3110 Δ*lsrR* and Δ*lsrK* strains appeared with significantly different structures than that of the wild type: an extracellular matrix not present on the wild type was observed on the surface of both mutants (Fig. 2). To investigate associated gene regulation, we carried out a complete transcriptome analysis of the *lsrR* and *lsrK* mutants and later reexamined biofilm formation using a more comprehensive flow cell chamber and confocal microscopy (see below).

***lsrR* and *lsrK* mutations reveal targets of AI-2 signaling.** For transcriptome analysis, cells were grown in LB medium (without glucose) to an OD_{600} of 2.4 ± 0.1 (early stationary phase). At this point, extracellular AI-2 in cultures of wild-type cells being transported back into the cells is nearly completely depleted from Δ*lsrR* mutants and is retained at near-peak levels in Δ*lsrK* mutants (69). To report the number of genes differentially expressed, we took the commonly used twofold ratio as a cutoff limit (11, 37), together with a P value of <0.05 to ensure statistical significance. Furthermore, a set of selected genes whose expression was changed by the *lsrR* and/or *lsrK*

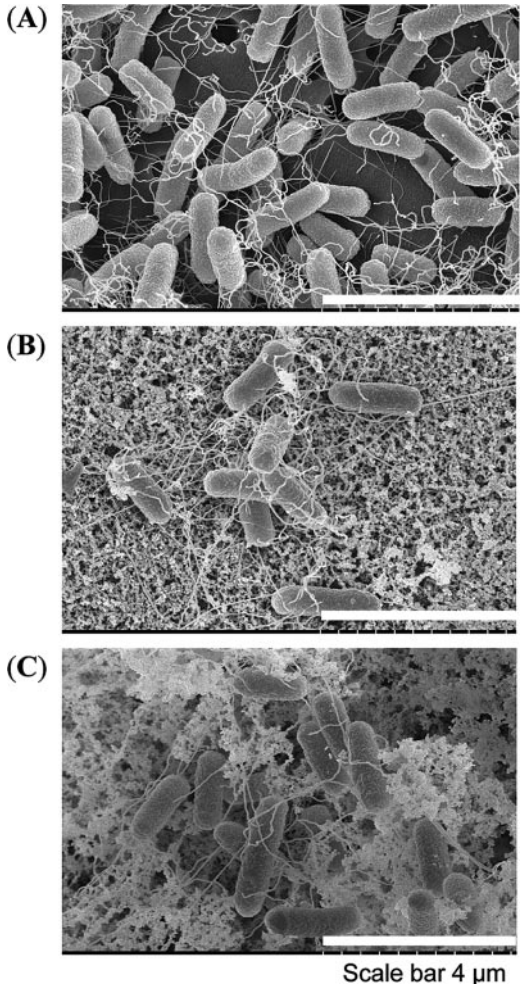

FIG. 2. Scanning electron micrographs of wild-type W3110 and isogenic *lsrR* and *lsrK* mutants. (A) Wild-type strain W3110. (B) Isogenic *lsrR* mutants. (C) Isogenic *lsrK* mutants. Length scale is indicated by bars.

gene was verified with real-time RT-PCR measurements. Figure 3 shows that there was a strong positive correlation (r^2 = 0.98 for *lsrR* mutants and r^2 = 0.96 for *lsrK* mutants) between the two techniques. Results indicate that there were 119 and 27 genes induced and repressed, respectively, at least twofold by *lsrR*, and there were 117 and 32 genes induced and repressed, respectively, by *lsrK*. Among these genes were 78 genes whose expression levels were changed by both *lsrR* and *lsrK* mutants (see Tables S1 to S3 in the supplemental material).

The coregulated genes comprise a number of genes that one might expect to be regulated by QS mechanisms. For example, *flu*, which encodes phase-variable protein antigen 43 (Ag43), was dramatically depressed, 10.8- and 6.3-fold in Δ*lsrR* and Δ*lsrK* mutants, respectively. Ag43 belongs to an autotransporter protein family, which regulates its own transport to the bacterial cell surface. Ag43 mediates cell-to-cell aggregation and thus enhances biofilm formation (16, 39, 53). As Ag43 plays an important role in the initial recognition and attachment to host tissue surfaces, it also plays a role in the pathogenesis of disease-causing *E. coli* (33). We carried out an

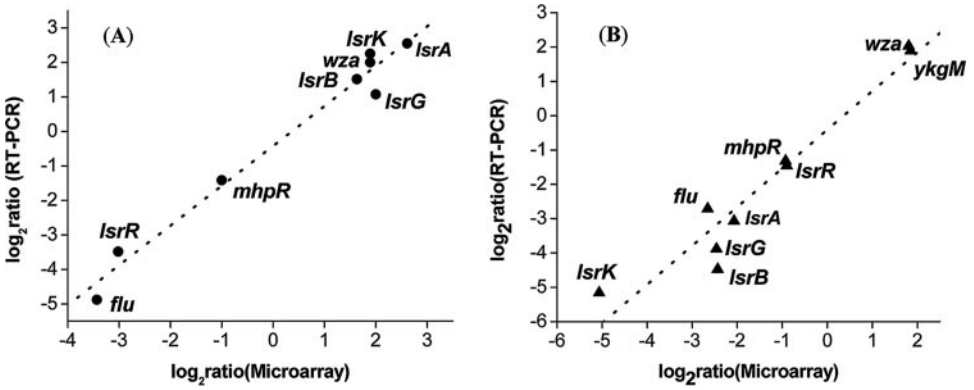

FIG. 3. Correlation between microarray and real-time RT-PCR results. The differences in expression of eight *lsrR*-controlled genes and nine *lsrK*-controlled were $\log_2$ transformed and plotted (microarray versus real-time RT-PCR). (A) Symbols: ●, W3110 Δ*lsrR*; dashed line, corresponding linear correlation between microarray data and real-time RT-PCR results. (B) Symbols: ▲, W3110 Δ*lsrK*; dotted line, corresponding linear correlation between microarray data and real-time RT-PCR results.

autoaggregation assay to see if *lsrRK* in fact played a role in aggregation, presumably through Ag43. An additional test between ZK2686 and its isogenic (Δ*flu*) mutant, ZK2692, was run to validate our assay as an indicator of Ag43 function. In Fig. 4, more wild-type cells settled to the bottom of the tubes, and faster, than both mutant strains (Fig. 4A), even though complete resolution of the assay took 2 days (Fig. 4B). We suspect that fimbrial blockage of autoaggregation may have contributed to this delay (32). The complete deficiency in autoaggregation of both *lsrR* and *lsrK* mutants is consistent with our microarray results and a regulatory model involving LsrR and LsrK.

There were 68 genes whose expression changed in an *lsrR* mutant alone (not changed in the *lsrK* mutant), and among these, 25 are hypothetical proteins with unknown function (see Table S2 in the supplemental material). We report a preponderance of genes associated with attachment, defense, and pathogenicity affected by the *lsrR* mutation. For example, a curli production assembly/transport component, *csgE*, from the second curli operon was repressed in the *lsrR* mutant. Curli is associated with biofilm formation, host cell adhesion and invasion, and immune system activation, where CsgA is the major fiber subunit and CsgE, CsgF, and CsgG are nonstructural proteins involved in curli biogenesis (4, 54). *htrE*, a homolog of *papD* involved in type II pilus assembly (51), was negatively regulated. Another putative fimbria-like protein, from b0942, was likely upregulated (twofold increase in expression in the *lsrR* mutant). A transmembrane domain, *sapB* of the SapABCD system (homologs of the *S. enterica* serovar Typhimurium SapABCD proteins) (49), which is required for virulence and resistance to the antimicrobial peptides melittin and protamine, was repressed in the *lsrR* mutant. Meanwhile, an increase in the transcription of a protamine-like protein, *tpr*, was observed. *yheF* (also called GspD), which belongs to a secretin protein family and is involved in virulence and filamentous phage extrusion (28), was upregulated by the *lsrR* deletion. YheF proteins are not normally expressed and are silenced by the nucleoid-structuring protein H-NS (26). The upregulation of *yheF* due to the *lsrR* deletion is likely an example of bacterial self-protection.

There were 71 genes whose expression changed in an *lsrK* mutant only, and among these genes, 38 are annotated as being

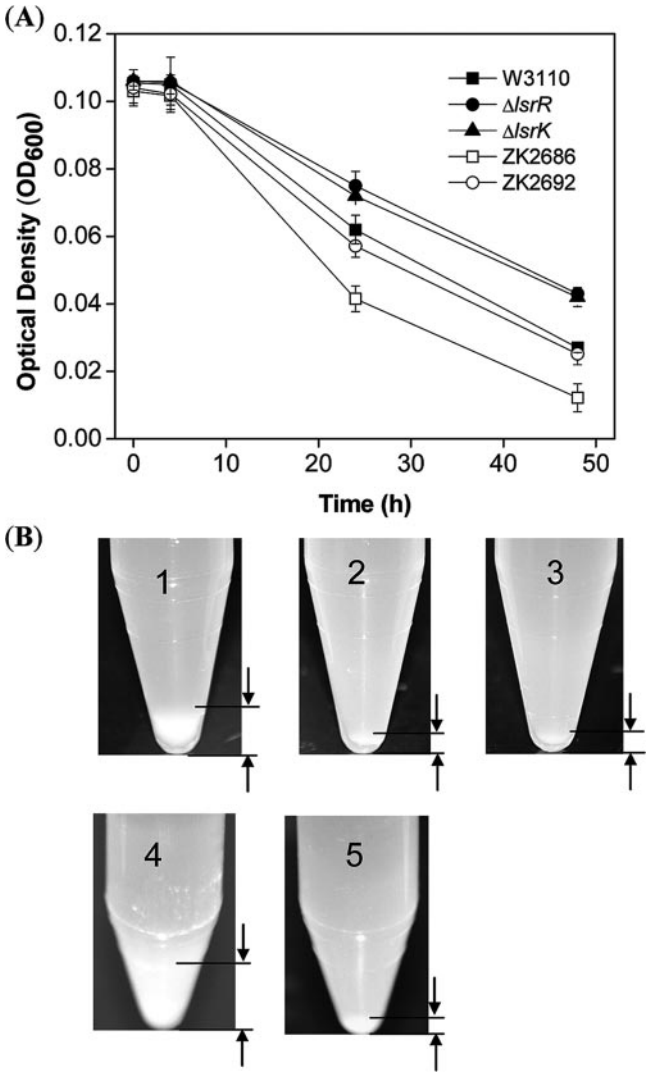

FIG. 4. Autoaggregation assay of W3110 and isogenic mutants Δ*lsrR* and Δ*lsrK*. (A) Time-resolved sedimentation results (autoaggregation assay) (see Materials and Methods). Symbols: ■, W3110; ●, W3110 Δ*lsrR*; ▲, W3110 Δ*lsrK*; □, ZK2686; ○, Δ*agn43* (isogenic mutant from parent strain ZK2686, called ZK2692). (B) Pictures of final pellets from the autoaggregation assay (A). 1, W3110; 2, W3110 Δ*lsrR*; 3, W3110 Δ*lsrK*; 4, ZK2686; 5, ZK2692.

TABLE 1. Biofilm-related genes from genomic profiling

Locus tag	Gene	Gene product	Fold change[a]	
			Δ*lsrR*/WT	Δ*lsrK*/WT
b2000	*flu*	Outer membrane fluffing protein, similar to adhesin	−10.8	−6.3
b2062	*wza*	Putative polysaccharide export protein	3.7	3.5
b0139	*htrE*	Probable outer membrane porin protein involved in fimbrial assembly	−3.2	
b1039	*csgE*	Curli production assembly/transport component, second curli operon	−3.0	
b0942		Putative fimbria-like protein	2.2	
b2059	*wcaA*	Putative regulator	3.5	
b0141	*yadN*	Putative fimbria-like protein		−2.0
b0136	*yadK*	Putative fimbrial protein		−2.4

[a] WT, wild type.

hypothetical proteins with unclear functions (see Table S3 in the supplemental material). Like *lsrR*, a number of genes associated with attachment, defense, and pathogenicity were found to be regulated by *lsrK*. *ppdD*, which encodes a putative major type IV pilin, was repressed twofold in an *lsrK* mutant. PpdD was able to form type IV pili when expressed in *Pseudomonas aeruginosa*, as determined by immunogold labeling (55). PpdD also formed pili when pullulanase secretion proteins from *Klebsiella oxytoca* and *E. coli* K-12 *ppdD* were coexpressed in *E. coli* (56). Genes for two putative fimbrial proteins, *yadK* and *yadN*, were repressed 2.4- and 2-fold, respectively, in the *lsrK* mutant. *mcrA*, a type IV site-specific DNase defending cells against foreign DNA such as bacteriophages (3), was upregulated 2.4-fold. *sieB*, similar to a λ gene responsible for preventing phage superinfection (25), was also upregulated 2.5-fold.

***lsrR* and *lsrK* regulate biofilm architecture and formation.** It is known that that flagella, fimbriae, type I pili, curli fibers, Ag43, exopolysaccharides (EPS), and other outer membrane adhesins are critical for biofilm development in *E. coli* (16, 17, 50, 53). However, several flagellum-related and motility-associated genes, such as the motility master regulon *flhDC* and type I adhesin, were unchanged in the *lsrR* and *lsrK* mutants compared to the parental strain. The complex nature by which EPS and capsular polysaccharides (CPS) exert influence on biofilm formation cannot be overstated, however. For example, in *Pseudomonas aeruginosa* and *V. cholerae*, QS is shown to control biofilm formation, in part, through the regulation of EPS synthesis (18, 30). Colanic acid synthesis is necessary for forming EPS and CPS during biofilm development (17, 48, 50). The product of the *wza* gene is associated with colanic acid synthesis for EPS and CPS surface expression and assembly (6, 23, 24, 47, 52, 72). Many reports have described the importance of *wza* in biofilm formation, and changes in *wza* expression affect biofilm formation (17, 48, 50). Remarkably, this gene was induced 3.7- and 3.5-fold in *lsrR* and *lsrK* mutants, respectively. Also, a putative regulator for colanic acid synthesis, *wcaA*, was induced 3.5-fold in *lsrR* mutants.

Another biofilm-related gene, *flu*, an autotransporter, was significantly repressed in both mutants (Table 1). The biofilm-related curli gene *csgE* and a putative fimbrial assembly gene, *htrE*, were both downregulated upon *lsrR* deletion. In *lsrK* mutants, two putative fimbria-related genes, *yadK* and *yadN*, were downregulated more than twofold. Our SEM analysis revealed significant differences in cell-based fimbriae and matrices of both mutants compared to the wild type (Fig. 2).

In order to further elucidate the variation in biofilm formation between the wild type and mutants, we utilized confocal scanning microscopy on flow-cell-derived biofilms (see Materials and Methods). Confocal images (Fig. 5) show for the first time that more biofilm was formed at the substrate surface in both mutant strains than in the wild type. Also, Imaris imaging demonstrated that the biofilm thicknesses of the *lsrR* and *lsrK* mutants were similar and much less than that of the wild type. Hence, the mean thickness and biomass of the wild type were higher, while the substratum coverage was lower than that of the mutants (Table 2) (because more of the mutant biofilms adhered to the bottom); that is, the bottom layer adjacent to the substrate appeared to be more substantive in the case of the mutants, and they tended to collapse and pack tightly onto the surface of the substrate.

In summary, two key functions known to affect biofilm formation and architecture, colanic acid synthesis and fimbria formation, were shown to be regulated by genes of the QS regulators LsrR and LsrK. Also, biofilm structures were altered significantly in the *lsrR* and *lsrK* mutants.

Deletion of *lsrR* and *lsrK* affected sRNA expression. As shown recently by Lenz and colleagues, small RNA (sRNA) species are involved in QS (42). We searched the intergenic regions for known and putative sRNAs (Table 3) and found that the global sRNA regulator DsrA was induced 3.6- and 4.4-fold in Δ*lsrR* and Δ*lsrK* strains, respectively. DsrA is a riboregulator for RpoS and H-NS production, wherein DsrA enhances the translation of *rpoS* RNA by stabilizing *rpoS* mRNA. It also inhibits H-NS translation by sharply increasing *hns* mRNA turnover (40, 44) and thereby curtails H-NS-mediated transcriptional silencing. Correspondingly, DsrA RNA also affects CPS biosynthesis via increased production of the activator RcsA due its inhibitory effects on H-NS-mediated transcriptional silencing (58). DsrA also plays a regulatory role in acid resistance (41). The regulatory effects of DsrA are mediated by specific RNA-to-RNA pairing interactions, while its stability and activity require the recruitment of Hfq (8, 46, 59, 60).

Since RpoS and H-NS play an important role in globally regulating genes in response to changing environments, it is not surprising that AI-2-related QS networks utilize their uptake regulators (e.g., LsrR and LuxP), together with DsrA, in a hierarchical modality for mediating prompt responses to environmental stimuli and extracellular stresses. Induction of components (*yheE* and *yheF*) in the type II secretion complex GspC to GspO is a good example of DsrA regulation: type II secretion was silenced by H-NS in wild-type *E. coli* (26), while

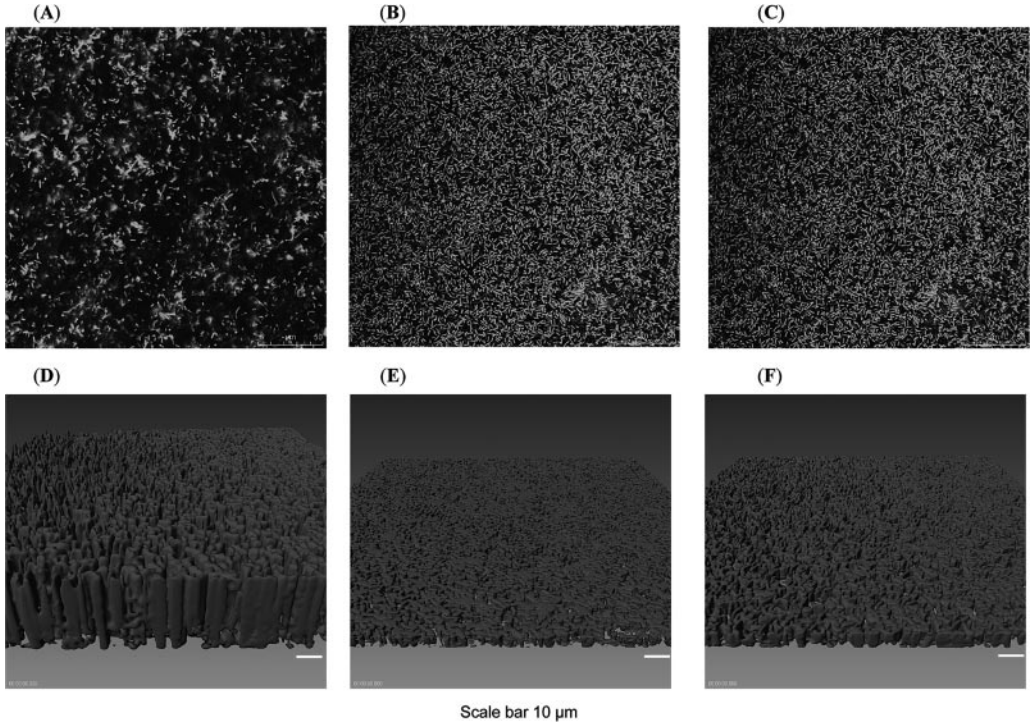

FIG. 5. Scanning confocal laser microscopic images of flow-cell-generated biofilms. (A and D) Wild-type W3110. (B and E) Isogenic *lsrR* mutant. (C and F) Isogenic *lsrK* mutant. We note that results for the *lsrR* mutant had a larger standard deviation than those for the *lsrK* mutant; the biofilm height was observed to fluctuate in the flow chamber (not shown here). A, B, and C are scanning confocal microscopic images; D, E, and F are reconstructed three-dimensional biofilm structures. The length scale is indicated by bars.

DsrA antagonizes the H-NS-mediated silencing of numerous promoters (58). Therefore, the QS-mediated induction of DsrA resulting from the *lsrR* and *lsrK* deletions leads to amplified expression of *yheE* and *yheF* (seemingly in the *lsrR* mutant only).

The sRNA cell division inhibitor DicF was induced by at least twofold in both *lsrR* and *lsrK* mutants. A twofold increase in expression of the cell division gene *dicB* was also observed, which is not surprising since both genes belong to the same cell division operon (see the supplemental material) (Table 1) (7). *dicF* inhibits cell division in *E. coli* by decreasing the abundance and activity of FtsZ; therefore, DicF affects the septum formation and separation of the replicated chromosomes into daughter nucleoids (63, 64). However, this inhibition effect can be suppressed by an *rpoB* mutation, and the inhibition effect is partially counteracted by an *rpoS* mutation (9). We note, however, that we did not see elongated cells in *lsrR* and *lsrK* mutants in our SEM studies. This is probably because cell division is a complex process controlled by many modes of regulation (1, 12, 29, 67).

Another sRNA immediately upstream of the *flu* gene was repressed in both mutants. This might account for the dramatic decrease in *flu* expression, 10.8- and 6.3-fold, respectively, in the *lsrR* and *lsrK* mutants described above, although a monocistronic RNA has not been identified. Two other sRNAs were found to be coregulated by *lsrR* and *lsrK*: one is *ayjiW*, and the other, which is unnamed, is located between *yfdI* and *tfaS*. The function of these riboregulators remains unclear and awaits further research.

The remaining sRNAs revealed in our study (Table 3) include three from the *lsrR* deletion (RydB, MicC, and Tpke70) and one from the *lsrK* deletion (SokX). High-copy expression of RydB decreases *rpoS* expression during the stationary phase in LB medium (71). It is intriguing to speculate that LsrR associates with RydB to assist in fine-tuning QS circuitry through the regulation of the global regulator RpoS. MicC works similarly as an antisense mechanism and is induced when cells are grown at low temperatures or in minimal medium (13). MicC negatively regulates the translation of an outer membrane protein, OmpC (14). Consistent with this posttranscriptional regulation, we did not see transcriptional changes in *ompC* expression or changes in the expression of its

TABLE 2. Confocal analysis report of biofilm flow cell assay

Strain	Biomass ($\mu m^3/\mu m^2$)	Substratum coverage (%)	Mean thickness (μm)	Roughness coefficient
W3110 type/pCM18	32.02 ± 3.2	20.4 ± 6.4	25.45 ± 2.8	0.196 ± 0.08
Δ*lsrK*:Kan^r/pCM18	3.64 ± 1.05	50.8 ± 4.7	2.95 ± 1.24	0.235 ± 0.05
Δ*lsrR*:Kan^r/pCM18	13.43 ± 14.43	44.6 ± 21.4	10.86 ± 11.85	0.229 ± 0.11

TABLE 3. sRNAs affected by *lsrR* and *lsrK*

Protein	Position		Flanking gene	Fold change[a]		Condition
	Start	End		Δ*lsrR*/WT	Δ*lsrK*/WT	
DsrA	2023233	2023532	*dsrB*/*yedP*	3.6	4.4	Confirmed
DicF	1647459	1647632	*rzpQ*/*dicB*	2.0	2.5	Confirmed
RydB/tpe7	1762411	1762957	*sufA* (*ydiC*)/*ydiH*	4.9		Confirmed
IS102	2069234	2069404	*yeeP*/*flu*	−2.3	−1.5	Confirmed
Tpke70	2494586	2496690	*ddg*/*yfdZ*	2.0		Confirmed
MicC (ISO63)	1434918	1435283	*ompN*/*ydbK*	3.2		Confirmed
AyjiW	4577468	4577637	Opposite *yjiW*	2.5	2.1	Confirmed
SokX	2885243	2885600			3.5	Confirmed
Unknown	2468480	2468778	*yfdI*/*tfaS*	2.3	3.2	Predicted

[a] WT, wild type.

regulator, *ompF*. Finally, Tpke70 is an antisense RNA with an unknown function. In *lsrK* mutants, SokX, of unknown function, was induced 3.5-fold.

DISCUSSION

In contrast to our previous microarray study of W3110 and a *luxS* mutant strain, LW7, where fewer than 50 genes were significantly affected by *luxS* mutation (70), our current study found many genes that were significantly affected by the *lsrR* and *lsrK* deletion (146 and 149 genes, respectively). Of these genes, only nine were regulated in exactly the same manner as that described previously for LuxS-regulated genes (Fig. 1) (70, 75). Deletion of *lsrR* results in the induction of the *lsr* operon (including the *lsrACDBFG* and *tam* genes), while deletion of *lsrK* results in the depression of those genes; that is, upon entry into the cell via the Lsr transporter, AI-2 is phosphorylated by LsrK. Phospho-AI-2 can bind the cognate transcriptional regulator LsrR and derepress gene expression. The immediate targets of this derepression are the very same AI-2 uptake genes (Fig. 1). Observations that AI-2 regulates its own uptake and transcriptome results indicating that few genes are impacted by the *luxS* mutation (70) have fueled speculation that AI-2 is limited in its role as a signal molecule in *E. coli*. Indeed, in our previous report, we suggested that the signaling role of AI-2 might require additional cellular factors (70).

A significant difference between the present *lsrR* and *lsrK* mutants and the *luxS* mutant is in the roles of the expressed proteins: signal perception versus signal generation. The present study enables a linkage between *lsrR* and *lsrK* to AI-2 as a signaling molecule. A key to this understanding was revealed previously but not reported for its importance (69, 70): the *lsr-lacZ* and *lsrR-lacZ* reporters in *lsrR* and *lsr* operon mutants were both upregulated manifold in both strains. Of note, the *lsr* transcription rate in an *lsr* operon mutant was upregulated to an almost equivalent extent to that in an *lsrR* mutant strain, suggesting that the cells still possessed phospho-AI-2 even though they did not possess the uptake complex. These cells did import AI-2 but at a much slower rate than the wild type and *lsrR* mutants. The same transcriptional reporter plasmid was nearly completely inactive in the *lsrK* mutant, as expected (consistent with the absence of derepression afforded by phospho-AI-2). Interestingly, the extracellular AI-2 level in LsrK mutants never dropped, suggesting that AI-2 was not taken up by the cells in the absence of LsrK. These results suggest that AI-2, taken in by an alternative transporter (alluded to in reference 70) or otherwise unsecreted AI-2, may still be phosphorylated by LsrK. These findings also suggest that (i) the Lsr transporter does not function without LsrK and (ii) LsrK can work with another transporter. These findings also give rise to the possibility that LsrK (and LsrR) may work on genes other than the *lsr* operon.

Indeed, the present analysis reveals a host of genes regulated by LsrR and LsrK, most of which did not appear in *luxS* mutants. Perhaps the most striking results of our current study are that (i) the majority of genes affected by the *lsrR* mutation are also affected by the *lsrK* mutation, (ii) the expression of the vast majority of these genes are identically affected (up or down) by both mutations, and (iii) these "coregulated" genes are not those of the *lsr* regulon (*tam*, *metE*, *yneE*, and *lsr* operons) (70). These findings suggest that AI-2, in addition to phospho-AI-2, is an LsrR regulator; that is, for the apparently coregulated genes, we suspect that a totally different regulatory mechanism than that shown in Fig. 1 exists (in which LsrR is a repressor [and at times an activator] and its repression is released by phospho-AI-2). We propose an extended hypothesis that LsrR is a QS regulator that acts in tandem with unphosphorylated AI-2 or its anomer (Fig. 6); namely, AI-2 binds to LsrR and derepresses the transcription of a variety of genes, those identified in Table S1 in the supplemental material, which one might expect should be under QS regulation (as opposed to metabolic genes associated with the activated methyl cycle) (70).

Our extended model is either supported by or consistent with all studies reported to date concerning AI-2, *luxS*, and *lsr* in *E. coli* and *Salmonella*. LsrR is a known transcriptional regulator that responds to the binding of QS signal AI-2 (62, 75). We suggest that the binding of phospho-AI-2 competes favorably with the binding of unphosphorylated AI-2 and that the interchange between AI-2 and phospho-AI-2 represents a switching mechanism for the affected genes. LsrR is transcribed in its own monocistronic operon with the kinase LsrK in a manner divergent from that of the *lsr* operon (70). It is therefore distinct from the uptake genes and can operate independently. AI-2 is internalized and phosphorylated by the Lsr/LsrK complex. We suggest this is the predominant mode of AI-2 entry into the cells and, by phosphorylation, prevents AI-2 efflux. However, AI-2 is taken up by Lsr mutants. Also, intracellular AI-2 by deletion of *ydgG* has been noted (35), and

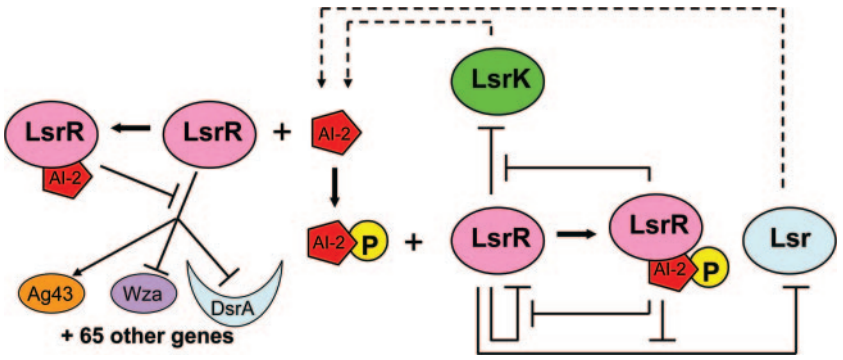

FIG. 6. Proposed AI-2 signaling with QS regulators LsrR and LsrK. During early and mid-exponential phases, AI-2 levels are low, insufficient for triggering rapid uptake. LsrR binds and represses many genes including *lsr* genes. As AI-2 accumulates extracellularly, it begins to be transported into the cells via a non-Lsr pathway or otherwise accumulates within the cells (or other pre-AI-2 anomers), which then bind to LsrR and derepress many QS genes including *lsrR*, *flu*, *wza*, and *dsrA* (crescents represent sRNA). Lsr-mediated AI-2 uptake remains repressed, as its derepression is due to phospho-AI-2. This temporal model is consistent with the activation of QS phenotypes that are switched on in late exponential phase. Finally, when the AI-2 concentration reaches the uptake "threshold" and cells sense nutrient depletion, *lsr* rapidly imports AI-2. Thereafter, cells phosphorylate the imported AI-2 signal, which results in the cessation of the LsrR/AI-2 regulation and amplification of LsrR/phopho-AI-2 regulation. Hence, a rapid QS switch is manifested by a change in the phosphorylation state of AI-2 and its binding to LsrR.

AI-2 is synthesized by non-LuxS/Pfs pathways (43). All are consistent with the existence of AI-2 (or its anomers) inside cells. An *lsrR* mutation leads to deficient LsrR expression and identification of LsrR-regulated genes. An *lsrK* mutation results in a lack of imported phospho-AI-2 (70), which is the principal signal for derepression of the *lsr* operon. We suggest that unphosphorylated AI-2 participates as a specific regulator of LsrR activity and that this mode of activity is the dominant feature of LsrR-mediated QS. We also suggest that the phosphorylated AI-2 acts as a "trigger" to terminate AI-2-mediated cellular processes and initiate the recycling of AI-2 through the *lsr* operon, which thus serves as the interconnect between the signaling process and a metabolic function. The metabolic functions of LuxS were described previously (70).

We prefer this signaling modality for AI-2-mediated QS for two reasons: first, QS signals have been shown to be global regulators, and hence, cells must have a purpose for importing and processing AI-2; second, *lsrR* and *lsrK* belong to an AI-2-mediated regulon (70). Thus, it is not surprising that *E. coli* utilizes the product of this operon to globally control the cellular phenotype. Our transcriptome results agree with this model, since most of the LsrRK-regulated genes are related to the cell's secretion systems (e.g., *flu* and *yheE*), biofilm formation (e.g., *wza*), transcriptional regulators (e.g., *mhpR*, *tdcA*, and *envR*), sRNAs or riboregulators (e.g., DsrA), and regulatory proteins for stress responses and nutrient depletion (e.g., *adiY*, *glnK*, and *cspF*). Indeed, AI-2 is perhaps a global regulator of *E. coli* (74) only when it is coupled to another regulator, as LuxP in *Vibrio harveyi*.

Our observation of biofilm phenotypes in *lsrR* and *lsrK* mutants cooperates with this model: AI-2 probably binds with LsrR to mediate biofilm architecture and formation by coordinately regulating interactions of biofilm-related genes, including the colanic acid synthesis regulator *wza* and the *flu* gene. Equally importantly, both of the genes affecting the phenotypes and the phenotypic outcomes were altered identically for the *lsrR* and *lsrK* strains. These findings suggest an intimate coordination between *lsrR* and *lsrK*, as shown in Fig. 6. The influence of these genes on biofilm structure has already been elucidated: their QS dependence is shown here for the first time.

Finally, our study provides the first evidence that sRNAs interact with QS regulators in *E. coli* K-12. A riboregulator, RsmZ, was found to control biofilm formation and type III secretion in *Pseudomonas aeruginosa* (66). Previous reports conclusively demonstrated that four sRNAs are intimately involved in the QS networks of *V. harveyi* and *V. cholerae* and act through the RNA chaperone Hfq (42). This finding is the first to suggest the convergence of an *E. coli* QS signaling system onto the Hfq/LuxO transduction process of *V. harveyi* and suggests yet one more modality for which bacterial autoinducer signal transduction occurs.

ACKNOWLEDGMENTS

We thank R. Kolter for generously providing strains ZK2686 and ZK2692 for our studies. We also thank A. Godínez for assistance in the DNA microarray experiments and T. Maugel for scanning electron microscopy experiments. We are grateful for proofreading by R. Fernandes.

This work was supported by the National Science Foundation (grants BES-0124401 and BES-0222687) and the U.S. Army.

REFERENCES

1. **Aarsman, M. E., A. Piette, C. Fraipont, T. M. Vinkenvleugel, M. Nguyen-Disteche, and T. den Blaauwen.** 2005. Maturation of the *Escherichia coli* divisome occurs in two steps. Mol. Microbiol. **55:**1631–1645.
2. **Ahmer, B. M.** 2004. Cell-to-cell signalling in *Escherichia coli* and *Salmonella enterica*. Mol. Microbiol. **52:**933–945.
3. **Anton, B. P., and E. A. Raleigh.** 2004. Transposon-mediated linker insertion scanning mutagenesis of the *Escherichia coli* McrA endonuclease. J. Bacteriol. **186:**5699–5707.
4. **Barnhart, M. M., and M. R. Chapman.** 2006. Curli biogenesis and function. Annu. Rev. Microbiol. **60:**131–147.
5. **Beeston, A. L., and M. G. Surette.** 2002. *pfs*-dependent regulation of autoinducer 2 production in *Salmonella enterica* serovar Typhimurium. J. Bacteriol. **184:**3450–3456.
6. **Beis, K., R. F. Collins, R. C. Ford, A. B. Kamis, C. Whitfield, and J. H. Naismith.** 2004. Three-dimensional structure of Wza, the protein required for translocation of group 1 capsular polysaccharide across the outer membrane of *Escherichia coli*. J. Biol. Chem. **279:**28227–28232.
7. **Bouche, F., and J. P. Bouche.** 1989. Genetic evidence that DicF, a second division inhibitor encoded by the *Escherichia coli dicB* operon, is probably RNA. Mol. Microbiol. **3:**991–994.
8. **Brescia, C. C., P. J. Mikulecky, A. L. Feig, and D. D. Sledjeski.** 2003. Identification of the Hfq-binding site on DsrA RNA: Hfq binds without altering DsrA secondary structure. RNA **9:**33–43.

9. **Cam, K., A. Cuzange, and J. P. Bouche.** 1995. Sigma S-dependent overexpression of *ftsZ* in an *Escherichia coli* K-12 *rpoB* mutant that is resistant to the division inhibitors DicB and DicF RNA. Mol. Gen. Genet. **248:**190–194.
10. **Camilli, A., and B. L. Bassler.** 2006. Bacterial small-molecule signaling pathways. Science **311:**1113–1116.
11. **Canales, R. D., Y. Luo, J. C. Willey, B. Austermiller, C. C. Barbacioru, C. Boysen, K. Hunkapiller, R. V. Jensen, C. R. Knight, K. Y. Lee, Y. Ma, B. Maqsodi, A. Papallo, E. H. Peters, K. Poulter, P. L. Ruppel, R. R. Samaha, L. Shi, W. Yang, L. Zhang, and F. M. Goodsaid.** 2006. Evaluation of DNA microarray results with quantitative gene expression platforms. Nat. Biotechnol. **24:**1115–1122.
12. **Chen, J. C., and J. Beckwith.** 2001. FtsQ, FtsL and FtsI require FtsK, but not FtsN, for co-localization with FtsZ during *Escherichia coli* cell division. Mol. Microbiol. **42:**395–413.
13. **Chen, S., E. A. Lesnik, T. A. Hall, R. Sampath, R. H. Griffey, D. J. Ecker, and L. B. Blyn.** 2002. A bioinformatics based approach to discover small RNA genes in the *Escherichia coli* genome. Biosystems **65:**157–177.
14. **Chen, S., A. Zhang, L. B. Blyn, and G. Storz.** 2004. MicC, a second small-RNA regulator of Omp protein expression in *Escherichia coli*. J. Bacteriol. **186:**6689–6697.
15. **Chen, Y. W., P. Zhao, R. Borup, and E. P. Hoffman.** 2000. Expression profiling in the muscular dystrophies: identification of novel aspects of molecular pathophysiology. J. Cell Biol. **151:**1321–1336.
16. **Danese, P. N., L. A. Pratt, S. L. Dove, and R. Kolter.** 2000. The outer membrane protein, antigen 43, mediates cell-to-cell interactions within *Escherichia coli* biofilms. Mol. Microbiol. **37:**424–432.
17. **Danese, P. N., L. A. Pratt, and R. Kolter.** 2000. Exopolysaccharide production is required for development of *Escherichia coli* K-12 biofilm architecture. J. Bacteriol. **182:**3593–3596.
18. **Davies, D. G., M. R. Parsek, J. P. Pearson, B. H. Iglewski, J. W. Costerton, and E. P. Greenberg.** 1998. The involvement of cell-to-cell signals in the development of a bacterial biofilm. Science **280:**295–298.
19. **De Keersmaecker, S. C., K. Sonck, and J. Vanderleyden.** 2006. Let LuxS speak up in AI-2 signaling. Trends Microbiol. **14:**114–119.
20. **DeLisa, M. P., and W. E. Bentley.** 2002. Bacterial autoinduction: looking outside the cell for new metabolic engineering targets. Microb. Cell Fact. **1:**5.
21. **DeLisa, M. P., J. J. Valdes, and W. E. Bentley.** 2001. Quorum signaling via AI-2 communicates the "metabolic burden" associated with heterologous protein production in *Escherichia coli*. Biotechnol. Bioeng. **75:**439–450.
22. **Domka, J., J. Lee, and T. K. Wood.** 2006. YliH (BssR) and YceP (BssS) regulate *Escherichia coli* K-12 biofilm formation by influencing cell signaling. Appl. Environ. Microbiol. **72:**2449–2459.
23. **Drummelsmith, J., and C. Whitfield.** 1999. Gene products required for surface expression of the capsular form of the group 1 K antigen in *Escherichia coli* (O9a:K30). Mol. Microbiol. **31:**1321–1332.
24. **Drummelsmith, J., and C. Whitfield.** 2000. Translocation of group 1 capsular polysaccharide to the surface of *Escherichia coli* requires a multimeric complex in the outer membrane. EMBO J. **19:**57–66.
25. **Faubladier, M., and J. P. Bouche.** 1994. Division inhibition gene *dicF* of *Escherichia coli* reveals a widespread group of prophage sequences in bacterial genomes. J. Bacteriol. **176:**1150–1156.
26. **Francetic, O., D. Belin, C. Badaut, and A. P. Pugsley.** 2000. Expression of the endogenous type II secretion pathway in *Escherichia coli* leads to chitinase secretion. EMBO J. **19:**6697–6703.
27. **Fuqua, W. C., S. C. Winans, and E. P. Greenberg.** 1994. Quorum sensing in bacteria: the LuxR-LuxI family of cell density-responsive transcriptional regulators. J. Bacteriol. **176:**269–275.
28. **Genin, S., and C. A. Boucher.** 1994. A superfamily of proteins involved in different secretion pathways in gram-negative bacteria: modular structure and specificity of the N-terminal domain. Mol. Gen. Genet. **243:**112–118.
29. **Hale, C. A., and P. A. de Boer.** 2002. ZipA is required for recruitment of FtsK, FtsQ, FtsL, and FtsN to the septal ring in *Escherichia coli*. J. Bacteriol. **184:**2552–2556.
30. **Hammer, B. K., and B. L. Bassler.** 2003. Quorum sensing controls biofilm formation in *Vibrio cholerae*. Mol. Microbiol. **50:**101–104.
31. **Hardie, K. R., C. Cooksley, A. D. Green, and K. Winzer.** 2003. Autoinducer 2 activity in *Escherichia coli* culture supernatants can be actively reduced despite maintenance of an active synthase, LuxS. Microbiology **149:**715–728.
32. **Hasman, H., T. Chakraborty, and P. Klemm.** 1999. Antigen-43-mediated autoaggregation of *Escherichia coli* is blocked by fimbriation. J. Bacteriol. **181:**4834–4841.
33. **Henderson, I. R., F. Navarro-Garcia, M. Desvaux, R. C. Fernandez, and D. Ala'Aldeen.** 2004. Type V protein secretion pathway: the autotransporter story. Microbiol. Mol. Biol. Rev. **68:**692–744.
34. **Henke, J. M., and B. L. Bassler.** 2004. Quorum sensing regulates type III secretion in *Vibrio harveyi* and *Vibrio parahaemolyticus*. J. Bacteriol. **186:**3794–3805.
35. **Herzberg, M., I. K. Kaye, W. Peti, and T. K. Wood.** 2006. YdgG (TqsA) controls biofilm formation in *Escherichia coli* K-12 through autoinducer 2 transport. J. Bacteriol. **188:**587–598.
36. **Houdt, R., A. Aertsen, P. Moons, K. Vanoirbeek, and C. W. Michiels.** 2006. *N*-Acyl-L-homoserine lactone signal interception by *Escherichia coli*. FEMS Microbiol. Lett. **256:**83–89.
37. **Ichikawa, J. K., A. Norris, M. G. Bangera, G. K. Geiss, A. B. van 't Wout, R. E. Bumgarner, and S. Lory.** 2000. Interaction of *Pseudomonas aeruginosa* with epithelial cells: identification of differentially regulated genes by expression microarray analysis of human cDNAs. Proc. Natl. Acad. Sci. USA **97:**9659–9664.
38. **Keller, L., and M. G. Surette.** 2006. Communication in bacteria: an ecological and evolutionary perspective. Nat. Rev. Microbiol. **4:**562.
39. **Kjaergaard, K., M. A. Schembri, C. Ramos, S. Molin, and P. Klemm.** 2000. Antigen 43 facilitates formation of multispecies biofilms. Environ. Microbiol. **2:**695–702.
40. **Lease, R. A., and M. Belfort.** 2000. A trans-acting RNA as a control switch in *Escherichia coli*: DsrA modulates function by forming alternative structures. Proc. Natl. Acad. Sci. USA **97:**9919–9924.
41. **Lease, R. A., D. Smith, K. McDonough, and M. Belfort.** 2004. The small noncoding DsrA RNA is an acid resistance regulator in *Escherichia coli*. J. Bacteriol. **186:**6179–6185.
42. **Lenz, D. H., K. C. Mok, B. N. Lilley, R. V. Kulkarni, N. S. Wingreen, and B. L. Bassler.** 2004. The small RNA chaperone Hfq and multiple small RNAs control quorum sensing in *Vibrio harveyi* and *Vibrio cholerae*. Cell **118:**69–82.
43. **Li, J., L. Wang, Y. Hashimoto, C. Y. Tsao, J. J. Valdes, T. K. Wood, E. Zafiriou, and W. E. Bentley.** 2006. A stochastic model of *Escherichia. coli* AI-2 quorum signal circuit reveals alternative synthesis pathways. Mol. Syst. Biol. **2:**1–16.
44. **Majdalani, N., C. Cunning, D. Sledjeski, T. Elliott, and S. Gottesman.** 1998. DsrA RNA regulates translation of RpoS message by an anti-antisense mechanism, independent of its action as an antisilencer of transcription. Proc. Natl. Acad. Sci. USA **95:**12462–12467.
45. **March, J. C., and W. E. Bentley.** 2004. Quorum sensing and bacterial cross-talk in biotechnology. Curr. Opin. Biotechnol. **15:**495–502.
46. **Moll, I., T. Afonyushkin, O. Vytvytska, V. R. Kaberdin, and U. Blasi.** 2003. Coincident Hfq binding and RNase E cleavage sites on mRNA and small regulatory RNAs. RNA **9:**1308–1314.
47. **Nesper, J., C. M. Hill, A. Paiment, G. Harauz, K. Beis, J. H. Naismith, and C. Whitfield.** 2003. Translocation of group 1 capsular polysaccharide in *Escherichia coli* serotype K30. Structural and functional analysis of the outer membrane lipoprotein Wza. J. Biol. Chem. **278:**49763–49772.
48. **O'Toole, G., H. B. Kaplan, and R. Kolter.** 2000. Biofilm formation as microbial development. Annu. Rev. Microbiol. **54:**49–79.
49. **Parra-Lopez, C., M. T. Baer, and E. A. Groisman.** 1993. Molecular genetic analysis of a locus required for resistance to antimicrobial peptides in *Salmonella typhimurium*. EMBO J. **12:**4053–4062.
50. **Prigent-Combaret, C., G. Prensier, T. T. Le Thi, O. Vidal, P. Lejeune, and C. Dorel.** 2000. Developmental pathway for biofilm formation in curli-producing *Escherichia coli* strains: role of flagella, curli and colanic acid. Environ. Microbiol. **2:**450–464.
51. **Raina, S., D. Missiakas, L. Baird, S. Kumar, and C. Georgopoulos.** 1993. Identification and transcriptional analysis of the *Escherichia coli htrE* operon which is homologous to *pap* and related pilin operons. J. Bacteriol. **175:**5009–5021.
52. **Reid, A. N., and C. Whitfield.** 2005. Functional analysis of conserved gene products involved in assembly of *Escherichia coli* capsules and exopolysaccharides: evidence for molecular recognition between Wza and Wzc for colanic acid biosynthesis. J. Bacteriol. **187:**5470–5481.
53. **Reisner, A., J. A. Haagensen, M. A. Schembri, E. L. Zechner, and S. Molin.** 2003. Development and maturation of *Escherichia coli* K-12 biofilms. Mol. Microbiol. **48:**933–946.
54. **Robinson, L. S., E. M. Ashman, S. J. Hultgren, and M. R. Chapman.** 2006. Secretion of curli fibre subunits is mediated by the outer membrane-localized CsgG protein. Mol. Microbiol. **59:**870–881.
55. **Sauvonnet, N., P. Gounon, and A. P. Pugsley.** 2000. PpdD type IV pilin of *Escherichia coli* K-12 can be assembled into pili in *Pseudomonas aeruginosa*. J. Bacteriol. **182:**848–854.
56. **Sauvonnet, N., G. Vignon, A. P. Pugsley, and P. Gounon.** 2000. Pilus formation and protein secretion by the same machinery in *Escherichia coli*. EMBO J. **19:**2221–2228.
57. **Sitnikov, D. M., J. B. Schineller, and T. O. Baldwin.** 1996. Control of cell division in *Escherichia coli*: regulation of transcription of *ftsQA* involves both *rpoS* and *sdiA*-mediated autoinduction. Proc. Natl. Acad. Sci. USA **93:**336–341.
58. **Sledjeski, D., and S. Gottesman.** 1995. A small RNA acts as an antisilencer of the H-NS-silenced *rcsA* gene of *Escherichia coli*. Proc. Natl. Acad. Sci. USA **92:**2003–2007.
59. **Sledjeski, D. D., C. Whitman, and A. Zhang.** 2001. Hfq is necessary for regulation by the untranslated RNA DsrA. J. Bacteriol. **183:**1997–2005.
60. **Sonnleitner, E., J. Napetschnig, T. Afonyushkin, K. Ecker, B. Vecerek, I. Moll, V. R. Kaberdin, and U. Blasi.** 2004. Functional effects of variants of the RNA chaperone Hfq. Biochem. Biophys. Res. Commun. **323:**1017–1023.
61. **Sperandio, V., A. G. Torres, B. Jarvis, J. P. Nataro, and J. B. Kaper.** 2003.

Bacteria-host communication: the language of hormones. Proc. Natl. Acad. Sci. USA **100:**8951–8956.
62. **Taga, M. E., S. T. Miller, and B. L. Bassler.** 2003. Lsr-mediated transport and processing of AI-2 in *Salmonella typhimurium*. Mol. Microbiol. **50:**1411–1427.
63. **Tetart, F., R. Albigot, A. Conter, E. Mulder, and J. P. Bouche.** 1992. Involvement of FtsZ in coupling of nucleoid separation with septation. Mol. Microbiol. **6:**621–627.
64. **Tetart, F., and J. P. Bouche.** 1992. Regulation of the expression of the cell-cycle gene *ftsZ* by DicF antisense RNA. Division does not require a fixed number of FtsZ molecules. Mol. Microbiol. **6:**615–620.
65. **Vendeville, A., K. Winzer, K. Heurlier, C. M. Tang, and K. R. Hardie.** 2005. Making 'sense' of metabolism: autoinducer-2, LuxS and pathogenic bacteria. Nat. Rev. Microbiol. **3:**383–396.
66. **Ventre, I., A. L. Goodman, I. Vallet-Gely, P. Vasseur, C. Soscia, S. Molin, S. Bleves, A. Lazdunski, S. Lory, and A. Filloux.** 2006. Multiple sensors control reciprocal expression of Pseudomonas aeruginosa regulatory RNA and virulence genes. Proc. Natl. Acad. Sci. USA **103:**171–176.
67. **Vicente, M., and A. I. Rico.** 2006. The order of the ring: assembly of *Escherichia coli* cell division components. Mol. Microbiol. **61:**5–8.
68. **Walters, M., and V. Sperandio.** 2006. Quorum sensing in *Escherichia coli* and *Salmonella*. Int. J. Med. Microbiol. **296:**125–131.
69. **Wang, L., Y. Hashimato, C. Y. Tsao, J. J. Valdes, and W. E. Bentley.** 2005. Cyclic AMP (cAMP) and cAMP receptor protein influence both synthesis and uptake of extracellular autoinducer 2 in *Escherichia coli*. J. Bacteriol. **187:**2066–2076.
70. **Wang, L., J. Li, J. C. March, J. J. Valdes, and W. E. Bentley.** 2005. *luxS*-dependent gene regulation in *Escherichia coli* K-12 revealed by genomic expression profiling. J. Bacteriol. **187:**8350–8360.
71. **Wassarman, K. M., F. Repoila, C. Rosenow, G. Storz, and S. Gottesman.** 2001. Identification of novel small RNAs using comparative genomics and microarrays. Genes Dev. **15:**1637–1651.
72. **Whitfield, C., and A. Paiment.** 2003. Biosynthesis and assembly of group 1 capsular polysaccharides in *Escherichia coli* and related extracellular polysaccharides in other bacteria. Carbohydr. Res. **338:**2491–2502.
73. **Winzer, K., K. R. Hardie, and P. Williams.** 2003. LuxS and autoinducer-2: their contribution to quorum sensing and metabolism in bacteria. Adv. Appl. Microbiol. **53:**291–396.
74. **Xavier, K. B., and B. L. Bassler.** 2003. LuxS quorum sensing: more than just a numbers game. Curr. Opin. Microbiol. **6:**191–197.
75. **Xavier, K. B., and B. L. Bassler.** 2005. Regulation of uptake and processing of the quorum-sensing autoinducer AI-2 in *Escherichia coli*. J. Bacteriol. **187:**238–248.